

# Application of Fractional Calculus to the Modeling of the Complex Rheological Behavior of Polymers: From the Glass Transition to Flow Behavior. I. The Theoretical Model

M. E. Reyes-Melo, V. A. González-González, C. A. Guerrero-Salazar, F. García-Cavazos, U. Ortiz-Méndez

Programa Doctoral en Ingeniería de Materiales, Facultad de Ingeniería Mecánica y Eléctrica, Universidad Autónoma de Nuevo León, Avenida Universidad Sin/Número, Ciudad Universitaria, San Nicolás de los Garza, Nuevo León 66450, México

Received 17 April 2007; accepted 3 October 2007

DOI 10.1002/app.27435

Published online 11 January 2008 in Wiley InterScience (www.interscience.wiley.com).

**ABSTRACT:** A model based on the concept of fractional calculus is proposed for the description of the dynamic elastic modulus ( $E^* = E' + iE''$ , where  $E^*$  is the complex modulus,  $E'$  is the storage modulus, or real part of the complex modulus, and  $E''$  is the loss modulus, or imaginary part of the complex modulus) under isothermal and isochronal conditions for amorphous polymers, including both the glass transition process and the flow behavior. The differential equations obtained for this model, which we call the *extended fractional Zener model* (EFZM), have differential and/or integral operators of fractional order between 0 and 1. The application of the Fourier transform to the fractional

equation of the EFZM, the association of their parameters to the relaxation times of the cooperative or noncooperative molecular movements of polymer chains, and the isothermal and isochronal diagrams of  $E'$  and  $\tan \delta = E''/E'$  were evaluated. These theoretical diagrams were typical curves that clearly showed the glass-transition ( $\alpha$ -relaxation) and flow behavior. The EFZM will enable us to analyze the complex rheological behavior of amorphous polymers. © 2008 Wiley Periodicals, Inc. *J Appl Polym Sci* 108: 731–737, 2008

**Key words:** amorphous; glass transition; modeling; modulus; rheology

## INTRODUCTION

Polymer processing requires a complete understanding of the complex rheological behavior of polymers in a temperature range from subvitreous temperature to the terminal flow zone. However, because of the long-chain character of polymer molecules, polymers are viscoelastic materials with rheological behaviors characterized by nonexponential relaxation processes exhibited in numerous experiments, such as dynamic mechanical analysis (DMA),<sup>1–4</sup> dielectric spectroscopy,<sup>1,5–7</sup> quasielastic light scattering,<sup>8,9</sup> and specific heat measurements.<sup>1,3,7,10</sup> Relaxation processes are associated with molecular motions that lead to a new structural equilibrium with a low energy content. The process by which the polymeric macromolecules are rearranged under the application of an external force is characteristic of their

structure and morphology; it proceeds at a rate that increases with temperature. The morphology of these materials is very complex, which makes them very difficult to handle analytically. In this sense, the use of differential and integral operators of fractional order (fractional calculus) is an alternative.<sup>10–17</sup>

The goal of this work was the application of fractional calculus to model the complex rheological behavior of amorphous polymers over a wide temperature range, including both the glass-transition and flow behaviors (the terminal flow zone). Using this new fractional model, we can associate the molecular mobility of polymeric chains to the complex rheological behavior of polymers displayed in diagrams of the storage modulus ( $E'$ ), or real part of the complex modulus, and  $\tan \delta = E''/E'$ . We call this new model the *extended fractional Zener model* (EFZM) because it is an extension of the fractional Zener model (FZM), which only can describe the glass-transition process.<sup>15</sup>

Correspondence to: M. E. Reyes-Melo (mreyes@gama.fime.uanl.mx).

Contract grant sponsor: Programa de Apoyo a la Investigación Científica y Tecnológica, Universidad Autónoma de Nuevo León.

## APPLICATION OF FRACTIONAL CALCULUS TO RHEOLOGY

Fractional calculus is the branch of mathematics that deals with the generalization of integrals and derivatives of all real orders. The application of fractional cal-

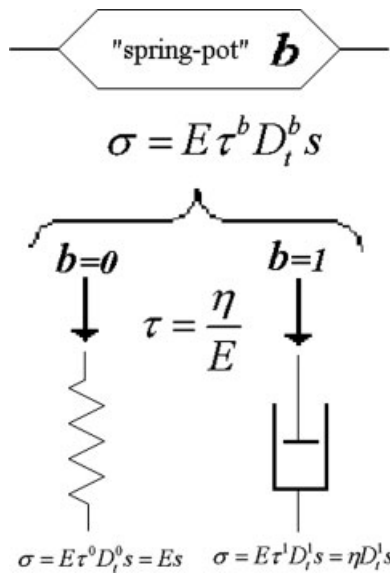


Figure 1 Spring-pot element.

culus to viscoelasticity is based on the fact that the spring and dashpot elements in the classical rheological models (Maxwell, Voigt–Kelvin, Zener, etc.) can be replaced by a spring-pot element.<sup>15–19</sup> The spring pot<sup>15,16</sup> combines the solid behavior (Hooke’s law) with fluid behavior (Newton’s law) by a differential operator of fractional order. Equation (1) corresponds to a spring pot; from this equation, one obtains Hooke’s law, or spring behavior, when parameter is the fractional order of the derivative of the deformation  $S$  with respect to time ( $b = 0$ ), and when  $b = 1$ , one obtains Newton’s law, or dashpot behavior (see Fig. 1):

$$\sigma = E^{1-b} \eta^b D_t^b S = E \left(\frac{\eta}{E}\right)^b D_t^b S = E \tau^b D_t^b S \quad 0 \leq b \leq 1 \quad (1)$$

where  $\sigma$  is the stress,  $S$  is the deformation,  $E$  is the elastic modulus,  $\eta$  is the viscosity, and  $\tau = \eta/E$  is a characteristic time called relaxation time, which can be associated with the time required by segment chains in motion for a complete reorganization and a full reorientation to a new structural equilibrium state. Finally,  $D_t^b S$  is the fractional derivative of the  $b$ th order of the deformation with respect to time.

It is important to remark here that the nonexponential relaxation process in polymers implies memory. A natural way to incorporate such memory effects is with formulations of noninteger order derivatives. Equation (2) represents the Riemann–Liouville derivative used in this work:<sup>15–22</sup>

$$D_t^b S(t) = D \int_0^t \frac{1}{\Gamma(1-b)} \frac{S(y) dy}{(t-y)^b} \quad b \in (0,1) \quad (2)$$

“ $y$ ” is a mathematical variable used in Riemann–Liouville derivative.

The Riemann–Liouville equation is calculated from eq. (3), which is a fractional integral defined between 0 and time ( $t$ ); in both eqs. (2) and (3),  $\Gamma$  is the gamma function:

$$D_t^{-b} S(t) = D \int_0^t \frac{1}{\Gamma(b)} \frac{S(y) dy}{(t-y)^{-b+1}} \quad b \in (0, \infty) \quad (3)$$

The fractional derivative [eq. (2)] represents a convolution integral in which the function  $S(t)$  is convolved with the impulse-response function of a  $b$ th-order fractional integrator. In this context, for eqs. (2) and (3), via the involved convolution integral, this state of the underlying system is influenced by all states at earlier times. On the other hand, from the point of view of physics, the fractional order of a fractional integral [eq. (3)] can be considered like an indication of the remaining energy of a signal passing through a viscoelastic material.<sup>16–22</sup> In similar way, the fractional order of a derivative [eq. (2)] reflects the rate at which a portion of the energy has been lost in the viscoelastic system.

Several authors have proposed the replacement of dashpots in rheological classical models with spring pots to afford an adequate description of relaxation processes deviating from exponential behavior.<sup>15–19</sup> The classical Zener model was modified by Alcoutlabi et al.<sup>15</sup> by the replacement of the dashpot by two spring pots for the modeling of the complex modulus ( $E^* = E' + iE''$ ) of an amorphous polymer.<sup>13,14</sup> However, this FZM can only describe the rheological behavior in a frequency ( $f$ ) or temperature range that corresponds to the glass-transition process. In more recent works,<sup>17,18</sup> it has been demonstrated that the FZM can be extended to model the complex rheological behavior of polymers with both the  $\alpha$ -relaxation (glass-transition) and secondary relaxations (observed at Temperature ( $T$ ) <  $T_g$ , where  $T_g$  is the glass-transition temperature) taken into account. Nevertheless, the flow behavior was not included in this model. In the next section, we describe the FZM that we extend for the modeling of complex rheological behavior, which includes both the glass-transition and flow behaviors (at  $T > T_g$ ).

## FZM

Figure 2 shows the FZM and the mathematical expression for  $E^*$  calculated from the fractional equation of the FZM. The first spring pot,  $a$ , has characteristically short relaxation times ( $\tau_a$ 's) associated with rheological behavior in the region at high  $f$  (or low temperature). The second spring pot,  $b$ , has characteristically long relaxation times ( $\tau_b$ 's) associated with rheological behavior in the region at low  $f$  (or high temperature), and the springs represent the elastic behavior of the polymers.<sup>15,17,18</sup>

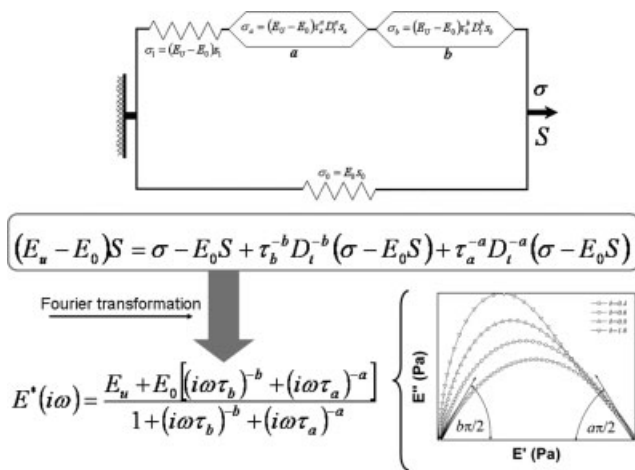


Figure 2 FZM with two spring pots.

$E^*$  calculated from the FZM is mainly a function of the angular frequency ( $\omega$  &  $2\pi f$ , where  $f$  is the frequency in Hz) of the alternating applied strain for DMA. In DMA,  $E'$  is in phase with the applied strain, and the loss modulus ( $E''$ ), or imaginary part of the complex modulus, is  $\pi/2$  out of phase with the strain. The phase lag ( $\delta$ ) between the strain and  $\sigma$  is defined as  $\delta = \tan^{-1}(\frac{E''}{E'})$ .

Also, in Figure 2 is shown a scheme of  $E'$  and  $E''$  in the complex plain. These curves, called *Cole-Cole diagrams*, enable us to estimate the fractional orders  $a$  and  $b$  of the FZM from experimental results.<sup>15-18</sup> In Cole-Cole diagrams, the slope angle at low values of  $E'$  will be  $b\pi/2$ , and in the region of high values of  $E'$  the angle will be  $a\pi/2$ . The Cole-Cole diagrams computed from FZM had classical asymmetric responses of the glass transition of polymer materials.<sup>15,16</sup> The shapes of these Cole-Cole curves confirmed the fact that the two spring-pot elements reproduced the rheological behavior corresponding to the glass transition at low and high  $f$  values.

Figure 3 shows theoretical diagrams of the  $f$  dependence of both  $E'$  and  $\tan \delta$  computed from FZM equations for several values of  $b$  and where  $a$  remained constant. At lower and high  $f$  values, the  $f$  dependence of  $E'$  and  $\tan \delta$  was negligible; at high  $f$  values,  $E' \approx E_U$  (where  $E_U$  is the unrelaxed modulus), and at low  $f$  values,  $E' \approx E_0$  (where  $E_0$  is the relaxed modulus). The intermediate region between  $E_U$  and  $E_0$  showed the typical mechanical manifestation of the glass transition by an increase of  $E'$  when  $f$  increased. This behavior was associated with a maximum value of  $\tan \delta$ , and the shape of the curves shown in Figure 3 was governed by both fractional parameters,  $a$  and  $b$ , as has been widely explained.<sup>15,17,18</sup>

Is important to remark here that the relaxation behavior described by the FZM by the replacement of the viscous element (dashpot) by two spring pots ( $a$  and  $b$ ) is a very good approximation of a non-exponential relaxation process. This relaxation phenomenon correspond to the glass-transition process (or  $\alpha$ -relaxation) of polymeric materials. Nevertheless, the secondary relaxations and the flow behavior cannot be described by the FZM.

In previous works,<sup>17,18</sup> we extended the FZM to model the glass transition ( $\alpha$ -relaxation) and the two secondary relaxations ( $\beta$  and  $\beta^*$  relaxations) of poly(ethylene 2,6 naphthalene dicarboxylate). The model proposed, which is based on three FZMs arranged in parallel, was called the *mechanical fractional model*. The first one poses two spring pots,  $a$  and  $b$ , associated mainly with  $\alpha$ -mechanic relaxation. The second one has only one spring pot,  $c$ , and it is associated with  $\beta^*$ -mechanic relaxation. The last one also has only one spring pot,  $d$ , associated with the mechanic manifestation of  $\beta$ . These results show that fractional calculus is a powerful tool for modeling the glass transition and the two secondary relaxations of poly(ethylene 2,6 naphthalene dicarboxylate); however, the flow behavior was not taken into account.

It is important to indicate that the FZM (Fig. 2) describes only the rheological behavior of the glass transition but is at variance with experimental behavior of uncrosslinked polymers in the terminal range, in which flow behavior can be observed at long times (or low  $f$  values). In the next section, we present the model proposed in this article (extending the FZM) for the modeling of both the glass-transition process and the flow behavior for amorphous polymers. In this work, the secondary relaxations are not taken into account.

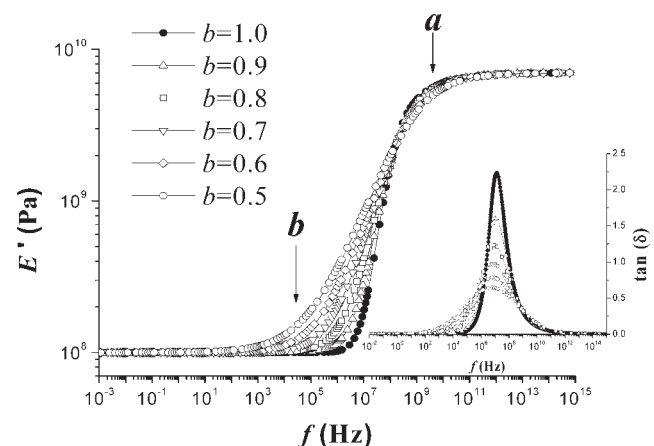


Figure 3  $f$  dependence of  $E'$  and  $\tan \delta = E''/E'$  described for the FZM with  $E_U = 7 \times 10^9$  Pa,  $E_0 = 1 \times 10^8$  Pa,  $\tau_a = 1.0 \times 10^{-9}$  s,  $\tau_b = 1.10 \times 10^{-9}$  s, and  $a = 0.4$ .

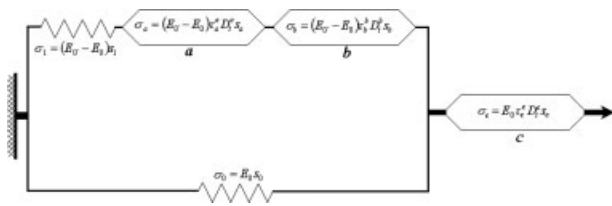


Figure 4 EFZM.

### EFZM

We added a spring-pot element to the FZM for the modeling of the glass-transition ( $\alpha$ -relaxation) and flow behavior in amorphous polymers. Figure 4 shows the proposed EFZM, and eq. (4) is the fractional equation of the EFZM. In the EFZM, spring

pot  $c$  represents the flow behavior of the polymer, and spring pots  $a$  and  $b$  are associated mainly with the glass-transition process:

$$E_U S + E_0 \tau_a^{-a} D_t^{-a} S + E_0 \tau_b^{-b} D_t^{-b} S = \sigma + \tau_a^{-a} D_t^{-a} \sigma + \tau_b^{-b} D_t^{-b} \sigma + \frac{E_U}{E_0} \tau_c^{-c} D_t^{-c} \sigma + \tau_a^{-a} \tau_c^{-c} D_t^{-a-c} \sigma + \tau_b^{-b} \tau_c^{-c} D_t^{-b-c} \sigma \quad (4)$$

Equation (4) provides, after Fourier transformation,  $E^*$  as a function of  $f$  and the parameters  $\tau_i(T)$ , where  $i = a, b$ , or  $c$ . The Fourier transform of a fractional operator  $[D_t^a f(t)]$  can be written as a product of  $(i\omega)^a$  and the Fourier transform of the function  $f(t)$ .<sup>15–22</sup> Equation (5) shows  $E^*$  calculated from eq. (4):

$$E^* = \frac{E_U + E_0 \tau_a^{-a} (i\omega)^{-a} + E_0 \tau_b^{-b} (i\omega)^{-b}}{1 + \tau_a^{-a} (i\omega)^{-a} + \tau_b^{-b} (i\omega)^{-b} + \frac{E_U}{E_0} \tau_c^{-c} (i\omega)^{-c} + \tau_a^{-a} \tau_c^{-c} (i\omega)^{-a-c} + \tau_b^{-b} \tau_c^{-c} (i\omega)^{-b-c}} \quad (5)$$

The mathematical expressions for  $E'$  and  $E''$  can be obtained from eq. (5).

$E'$  is calculated as

$$E'(\omega) = \frac{A_1 A_3 + A_2 A_4}{A_3^2 + A_4^2} \quad (6)$$

where  $A_1$ ,  $A_2$ ,  $A_3$ , and  $A_4$  are defined by the following equations:

$$A_1 = E_U + E_0 (\tau_a \omega)^{-a} \cos\left(a \frac{\pi}{2}\right) + E_0 (\tau_b \omega)^{-b} \cos\left(b \frac{\pi}{2}\right) \quad (7)$$

$$A_2 = -E_0 (\tau_a \omega)^{-a} \sin\left(a \frac{\pi}{2}\right) - E_0 (\tau_b \omega)^{-b} \sin\left(b \frac{\pi}{2}\right) \quad (8)$$

$$A_3 = 1 + (\tau_a \omega)^{-a} \cos\left(a \frac{\pi}{2}\right) + (\tau_b \omega)^{-b} \cos\left(b \frac{\pi}{2}\right) + \frac{E_U}{E_0} (\tau_c \omega)^{-c} \cos\left(c \frac{\pi}{2}\right) + \tau_a^{-a} \tau_c^{-c} (\omega)^{-a-c} \cos\left((a+c) \frac{\pi}{2}\right) + \tau_b^{-b} \tau_c^{-c} (\omega)^{-b-c} \cos\left((b+c) \frac{\pi}{2}\right) \quad (9)$$

$$A_4 = -(\tau_a \omega)^{-a} \sin\left(a \frac{\pi}{2}\right) - (\tau_b \omega)^{-b} \sin\left(b \frac{\pi}{2}\right) - \frac{E_U}{E_0} (\tau_c \omega)^{-c} \sin\left(c \frac{\pi}{2}\right) - \tau_a^{-a} \tau_c^{-c} (\omega)^{-a-c} \sin\left((a+c) \frac{\pi}{2}\right) - \tau_b^{-b} \tau_c^{-c} (\omega)^{-b-c} \sin\left((b+c) \frac{\pi}{2}\right) \quad (10)$$

With eqs. (7)–(10),  $E''$  is defined as

$$E''(\omega) = \frac{A_2 A_3 - A_1 A_4}{A_3^2 + A_4^2} \quad (11)$$

From eqs. (7)–(11), the theoretical diagrams of the  $f$  dependence (isothermal conditions) of  $E'$  and  $\tan \delta = E''/E'$  were computed with the consideration that at a constant temperature, the  $\tau_i$  parameters of EFZM are constants with the following behavior:  $\tau_c > \tau_b > \tau_a$ . The parameter  $\tau_c$  is associated with the long times required to displace molecular chains in the flow behavior, and  $\tau_b$  and  $\tau_a$  are the long and short times, respectively, they are associated with the molecular mobility in the glass transition as explained in refs. 15, 17, and 18. To calculate the  $f$  dependence of  $E'$  and  $\tan \delta$ , values of  $a = 0.4$ ,  $b = 0.7$ , and  $c = 0.9$  were arbitrarily selected. Figure 5 shows the isothermal diagrams obtained for  $E'(f)$

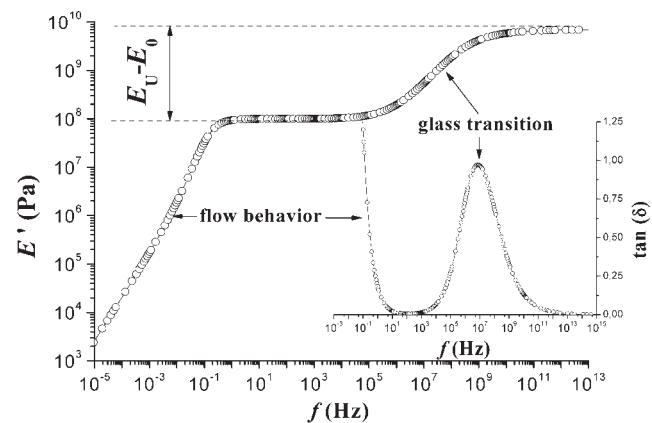


Figure 5  $f$  dependence of  $E'$  and  $\tan \delta = E''/E'$  described for EFZM with  $a = 0.4$ ,  $b = 0.7$ ,  $c = 0.9$ ,  $E_U = 7 \times 10^9$  Pa,  $E_0 = 1 \times 10^8$  Pa,  $\tau_a = 1 \times 10^{-9}$  s,  $\tau_b = 1.1 \times 10^{-9}$  s, and  $\tau_c = 1$  s.

and  $\tan \delta$  versus  $f$ . These theoretical diagrams correspond to the typical rheological behavior of an amorphous polymer (the glass-transition and flow behaviors). It is important to remark here that for semicrystalline polymers, the mechanical manifestation of the crystalline part must be displayed as a second peak on the  $\tan \delta$  diagram. This second peak must be located between the glass transition and the flow behavior, and it was not taken into account in this work.

Figure 5 shows that at high  $f$  values,  $E'$  does not depend on  $f$ , and the observed plateau is associated with the elastic behavior of the polymer; this is similar to a glassy state in which the polymer is very stiff and has a very high  $E_U$ . When  $f$  decreases,  $E'$  also decreases; this behavior is maintained until a  $f$  value where a second plateau of  $E'(f)$  appears and is related to rubberlike behavior. This important decrease in  $E'$  is equal to  $E_U - E_0$  and is associated with a maximum value on the  $\tan \delta$  diagram; this peak corresponds to the mechanical manifestation of the glass-transition process. Finally, at very slow  $f$  values, the flow behavior is obtained; in this case  $E'$  presents an important decrease when  $f$  decreases. This rheological behavior corresponds to an important increase in  $\tan \delta$ .

The mathematical representation of the  $f$  dependence of  $E'$  could be obtained by application of the Fourier transform to the EFZM. In practice, it is very useful to also describe the analysis of the temperature dependence of  $E'$  and  $\tan \delta$  (isochronal conditions). To obtain the isochronal diagrams of both  $E'$  and  $\tan \delta$  from the EFZM, first it was necessary to define the relationship between  $\tau$  and temperature ( $T$ ), which in turn, depends on the cooperative or noncooperative nature of the molecular mobility of polymers. The cooperative molecular movements are simultaneous motions at a time of segments of macromolecular chains due to the interference between neighboring segment chains.<sup>1,17,18</sup> When the temperature decreases, many segments of chains are involved in the cooperative process, the probability for this process is small, and  $\tau$  increases and tends toward an infinite value to the Kauzmann zero-entropy temperature ( $T_0$ ). The associated molecular mobility of the glass-transition ( $\alpha$ -relaxation) and flow behavior are typical examples of cooperative processes.<sup>1</sup> The  $\tau$  values for the cooperative movements verify a power law:<sup>1,15,17,18</sup>

$$\tau = \tau_0 \left( \frac{\tau}{\tau_0} \right)^Z \quad T_0 \leq T \leq T^* \quad (12)$$

where  $\tau$  is the relaxation time of the elementary or fasted molecular motions of cooperative movements, and it is defined by an Arrhenius equation:

$$\tau = \tau_0 \exp \left( \frac{E_a}{k_B T} \right) \quad (13)$$

where  $E_a$  is the activation energy identifiable with real energy barriers, which can be different for the cooperative movements in glass transition and for the cooperative movements in flow behavior, and  $k_B$  is the Boltzmann constant. The term  $\tau_0$  is a pre-exponential factor with values within the range  $10^{16}$  s  $\leq \tau_0 \leq 10^{13}$  s; values in the vicinity of the upper limit correspond to molecular vibrational times, and those near the lower limit may be rationalized as additional entropy contributions.<sup>1,2</sup> In eq. (12), the parameter  $Z$  is associated with the number of elementary movements participating in the cooperative process, and it depends on the polymer structure. The  $Z$  exponent is estimated with the next equation:

$$Z = \frac{T T^* - T_0}{T^* T - T_0} \quad T_0 \leq T \leq T^* \quad (14)$$

The temperature  $T^*$  is approximately  $1.3T_g$  for completely amorphous polymers, and it is a crossover temperature above which molecular movements are noncooperative.  $Z = 1$ ; in consequence, the  $\tau$  values follow an Arrhenius law [eq. (13)].

To verify the rheological behavior modeled by EFZM, in the next section, we proceed to vary systematically the fractional order of the spring pots for both isothermal and isochronal conditions. It is important to point out that the fractional parameters can only take values between 0 and 1.

### TESTING THE RESPONSE OF THE EFZM

Shown in Figure 6 are the predictions of  $E'$  and  $\tan \delta$  under isothermal conditions for different values of  $b$ ; the remaining parameters  $a$  and  $c$  are constants. Figure 7 shows the correspondent isochronal diagrams of  $E'$  and  $\tan \delta$  at  $f = 10$  Hz; in this case, the temperature dependence of  $\tau_a$ ,  $\tau_b$ , and  $\tau_c$  are defined by eqs. (12)–(14).

Figure 6 shows how both parameters  $b$  and  $a$  define the shape of the curves in a  $f$  range where the glass transition is observed. At very high  $f$  values, all curves are superposed because the  $a$  parameter is constant; the same effect is observed at very slow  $f$  values because, in this case, the  $c$  parameter, which defines the flow behavior, is also constant. On the other hand and also for a  $f$  of 10 Hz, we corroborated the effect of parameter  $b$  on the glass transition in the isochronal diagrams of  $E'$  and  $\tan \delta$ ; they are shown in Figure 7. In addition, shown in Figures 6 and 7 are the effects of the parameter  $b$  on the shape of the second plateau of  $E'$  associated with rubberlike behavior. The decrease in  $E'(f)$  when  $f$  decreases

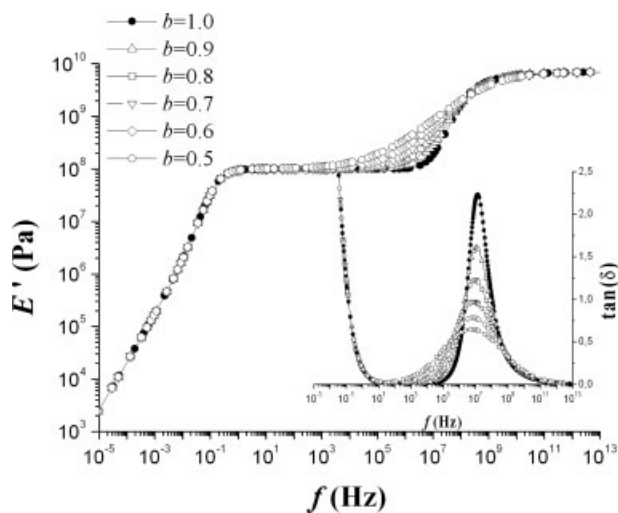


**Figure 6** Effect of the  $b$  parameter on the  $f$  dependence of  $E'$  and  $\tan \delta$  with  $a = 0.4$ ,  $c = 0.9$ , and the same values of  $E_U$ ,  $E_0$ ,  $\tau_a$ ,  $\tau_b$ , and  $\tau_c$  used in Figure 5.

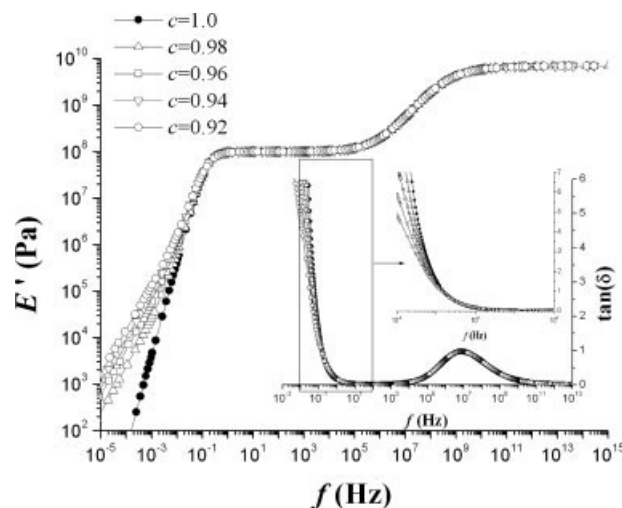


**Figure 8** Effect of the  $c$  parameter on the  $f$  dependence of  $E'$  and  $\tan \delta$  with  $a = 0.4$ ,  $b = 0.8$ , and the same values of  $E_U$ ,  $E_0$ ,  $\tau_a$ ,  $\tau_b$ , and  $\tau_c$  used in Figure 5.

[or the decrease in  $E'(T)$  when  $T$  increases] is more pronounced when  $b$  increases, and the second plateau associated with rubberlike behavior is greater. This behavior corresponds to an increase in the peak amplitude of  $\tan \delta$  when  $b$  increases. The presence of this second plateau is related to a critical molecular weight, above which entanglements exist and the shape of plateau could be associated with molecular weight polydispersity of the polymer. In this sense, Alcoutlabi et al.<sup>15</sup> and Friedrich et al.<sup>10</sup> used the fractional calculus concepts (spring pots) to compute the  $\tau$  spectra of polymers that could be related to molec-

ular weight polydispersity. On the other hand, the curves of Figures 6 and 7 show an equivalence high  $f$  values and low temperatures (or low  $f$  values and high temperatures). This behavior has been identified from experimental results obtained by DMA<sup>15,17,18</sup> for several polymers.

The parameter  $b$  thus affects the minima localized between the flow behavior and glass transition on the one hand and the peak amplitude of the glass transition on  $\tan \delta$  diagrams on the other hand.

From Figures 6 and 7, we corroborated that parameters  $b$  and  $a$  affect mainly the shape of curves in a region corresponding to the glass-transition process.

Figure 8 shows the effect of the  $c$  parameter under isothermal conditions for the  $E'$  and  $\tan \delta$  diagrams;

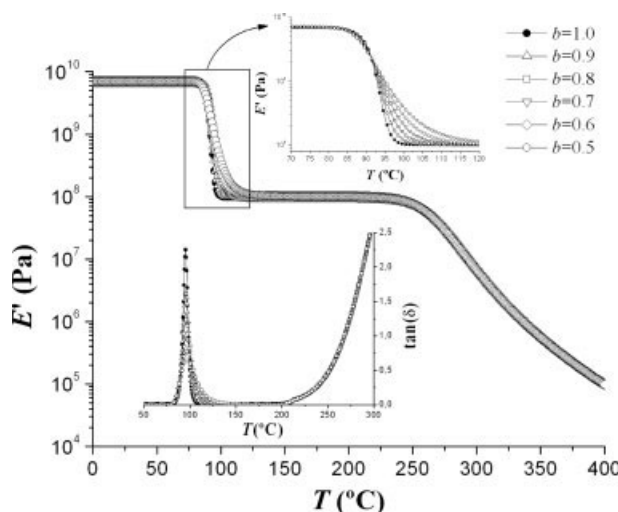


**Figure 7** Effect of the  $b$  parameter on the temperature dependence of  $E'$  and  $\tan \delta$  with  $a = 0.4$ ,  $c = 0.9$ , and the same values of  $E_U$  and  $E_0$  used in Figure 5. Parameters for the glass-transition process:  $\tau_b(T) = \tau_a(T)$ ,  $\tau_0 = 1 \times 10^{-14}$  s,  $E_a = 28.95$  kJ/mol,  $T^* = 485$  K, and  $T_0 = 323$  K. Parameters for the flow behavior:  $\tau_c(T)$   $\tau_0 = 1 \times 10^{-14}$  s,  $E_a = 125.45$  kJ/mol,  $T^* = 485$  K, and  $T_0 = 323$  K.

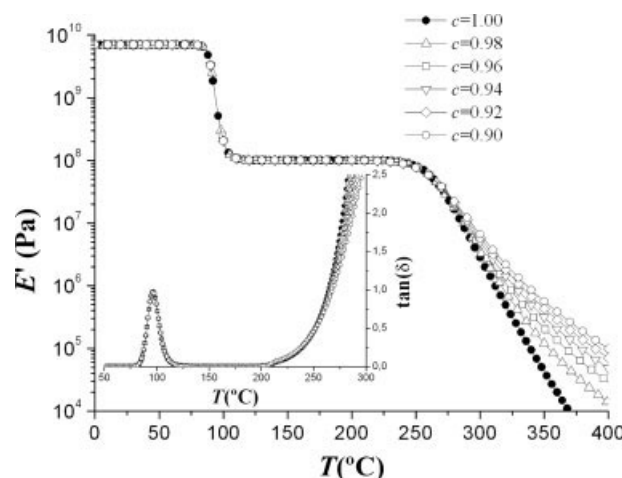


**Figure 9** Effect of the  $c$  parameter on the temperature dependence of  $E'$  and  $\tan \delta$  with the same values of  $E_U$  and  $E_0$  used in Figure 5. The parameters  $\tau_a$ ,  $\tau_b$ , and  $\tau_c$  are defined in Figure 7.

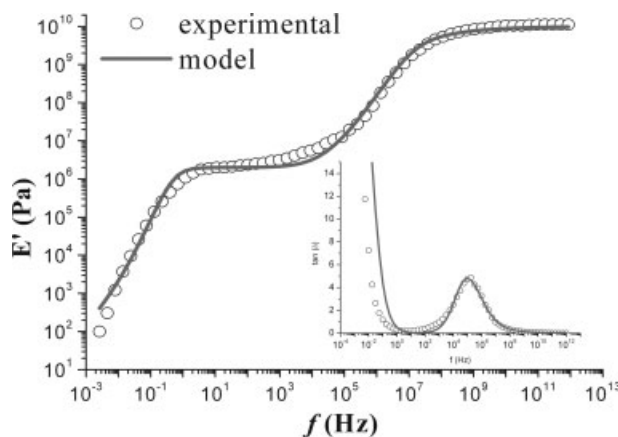


**Figure 10** Comparison of the model predictions and experimental data for a polystyrene specimen at  $T = 100^\circ\text{C}$ .

in this case, parameters  $a$  and  $b$  are constants. Figure 9 shows the correspondent isochronal diagrams of  $E'$  and  $\tan \delta$  at a  $f$  of 10 Hz.

Under isothermal conditions (Fig. 8), the flow behavior is identified at very low  $f$  values by a pronounced decrease in  $E'$  when  $f$  decreases, and under isochronal conditions (Fig. 9) is identified by a pronounced decrease in  $E'$  when the temperature increases. In both cases, the more pronounced decrease in  $E'$  was obtained when  $c = 1$ . In this case, spring pot  $c$  describes the rheological behavior of a dashpot (viscous pure liquid), and when  $c$  decreases, the flow behavior has a tendency to disappear.

In both cases (Figs. 8 and 9), parameter  $c$  affects mainly the rheological behavior of the terminal flow zone. The decrease in  $E'$  when  $f$  decreases or  $T$  increases is related to an increase in  $\tan \delta$  under isothermal and isochronal conditions.

In Figures 8 and 9, the curves in the region corresponding to glass transition are superposed because the  $a$  and  $b$  parameters remain constant, and we corroborated the equivalence high  $f$  values and low temperatures (or low  $f$  values and high temperatures) with the theoretical diagrams of  $E'$  and  $\tan \delta$ . Finally, the theoretical descriptions of the EFZM were compared with experimental results extracted from the literature.<sup>2</sup> As shown in Figure 10, good agreement between the model predictions and experimental results was obtained under isothermal conditions ( $T = 100^\circ\text{C}$ ) for a polystyrene specimen. The values of fractional parameters used to obtain the theoretical curves of Figure 10 are  $c = 0.98$ ,  $b = 0.92$ , and  $a = 0.33$ . In future work, we will analyze the experimental rheological behavior in a  $f$  or temperature range for amorphous polymers showing glass-transition and flow behaviors. This will enable us to associate a molecular interpretation to the fractional parameters of our EFZM.

## CONCLUSIONS

Theoretical diagrams obtained from the fractional equation of the EFZM describe the complex rheological behavior of amorphous polymers and display typical curves that clearly show the glass-transition and flow terminal zone.

Choosing in an arbitrary way the values of the fractional orders of the EFZM, we computed for a sinusoidal request  $E'$  and  $\tan \delta = E''/E'$  under isothermal conditions. The isochronal diagrams of  $E'$  and  $\tan \delta$  were computed with the temperature dependence of the  $\tau$  parameters considered. These theoretical diagrams enabled us to analyze the effect of the fractional parameters for the glass-transition and flow behaviors. We corroborated that the  $a$  and  $b$  parameters are associated mainly with the glass transition, and parameter  $c$  is associated with the flow behavior.

## References

1. Matsuoka, S. *Relaxation Phenomena in Polymers*; Hanser: Munich, 1992.
2. Ferry, J. D. *Viscoelastic Properties of Polymers*; Wiley: New York, 1980.
3. Angell, C. A.; Ngai, K. L.; McKenna, G. B.; McMillan, P. F.; Martin, S. W. *Appl Phys Rev* 2000, 88, 3113.
4. Gauthier, C.; Pelletier, J. M.; David, L.; Vigier, G.; Perez, J. *J Non-Cryst Solids* 2000, 274, 181.
5. Hakme, C.; Stevenson, I.; David, L.; Boiteux, G.; Seytre, G.; Schönhal, A. *J Non-Cryst Solids* 2005, 351, 2742.
6. Dantras, E.; Dudognon, E.; Samouillan, V.; Menegotto, J.; Bernès, A.; Demont, P.; Lacabanne, C. *J Non-Cryst Solids* 2002, 307–310, 671.
7. Cañadas, J. C.; Diego, J. A.; Sellarès, J.; Mudarra, M.; Belana, J.; Díaz-Calleja, R.; Sanchis, M. *J. Polymer* 2000, 41, 2899.
8. Savin, D. A.; Gary, D.; Patterson, G. D.; Stevens, J. R. *J Polym Sci Part B: Polym Phys* 2005, 43, 1504.
9. Lehman, S. Y.; McNeil, L. E.; Albalak, R. J. *J Polym Sci Part B: Polym Phys* 2000, 38, 2170.
10. Friedrich, C.; Braun, H.; Weesse, J. *Polym Eng Sci* 1995, 35, 1661.
11. Song, D. Y.; Jiang, T. Q. *Rheol Acta* 1998, 37, 512.
12. Hernández-Jiménez, A.; Hernández-Santiago, J.; Macías-García, A.; Sánchez-González, J. *Polym Test* 2002, 21, 325.
13. Pritz, T. *J Sound Vib* 2003, 265, 935.
14. Perez, J. *Matériaux Non Cristallins et Science du Désordre*; Presses Polytechniques et Universitaires Romandes; Lausanne, Switzerland, 2001.
15. Alcoutlabi, M.; Martínez-Vega, J. J. *Polymer* 2003, 44, 7199, and references therein.
16. Le Méhauté A.; Nigmatullin, R. R.; Nivanen, L. *Flèches du Temps et Géométrie Fractale*, 2nd ed.; Hermes: Paris, 1998.
17. Reyes-Melo, E.; Martínez-Vega, J. J.; Guerrero-Salazar, C.; Ortiz-Méndez, U. *J Appl Polym Sci* 2004, 94, 657, and references therein.
18. Reyes-Melo, M. E.; Martínez-Vega, J. J.; Guerrero-Salazar, C. A.; Ortiz-Méndez, U. *J Appl Polym Sci* 2006, 102, 3354, and references therein.
19. Heymans, N.; Podlubny, I. *Rheol Acta* 2006, 45, 765.
20. Moshrefi-Torbati, M.; Hammond, K. *J Franklin Inst B* 1998, 335, 1077.
21. Heymans, N. *Signal Process* 2003, 83, 2345.
22. Hilfer, R. *Fractals* 2003, 11, 251.